Examining the Role of Hydrogen Bonding Interactions in the Substrate Specificity for the Loading Step of Polyketide Synthase Thioesterase Domains[†]

Meng Wang and Christopher N. Boddy*

Department of Chemistry, Syracuse University, Syracuse, New York 13244-4100

Received May 21, 2008; Revised Manuscript Received September 3, 2008

ABSTRACT: The final step in polyketide synthase-mediated biosynthesis of macrocyclic polyketides is thioesterase (TE)-catalyzed cyclization of a linear polyketide acyl chain. TEs are highly specific in the chemistry they catalyze. Understanding the molecular basis for substrate specificity of TEs is crucial for engineering these enzymes to macrocyclize non-native linear substrates. We investigated the role of hydrogen bonding interactions in the substrate specificity of formation of an acyl−enzyme intermediate for the TE from the 6-deoxyerythronolide B biosynthetic pathway. Thirteen single site-directed mutants were constructed, via removal of side chain hydrogen bonding groups from the binding cavity. Specificity constants for four different substrates with and without hydrogen bond donors and acceptors were determined for the five active mutants. The relative magnitude of specificity constants for substrates did not change for the mutant TEs. Circular dichroism spectroscopy was used to show that the majority of the catalytically inactive mutants did not fold. Two mutations were identified that enabled mutant TEs to form a folded but catalytically inactive tertiary structure. Our data do not support a role for hydrogen bonding in mediating substrate specificity of bacterial polyketide synthase TEs. The highly conserved polar residues in the binding cavity appear to stabilize the unusual substrate channel, which passes through the enzyme. We propose that hydrophobic interactions between the binding cavity and substrate drive substrate specificity, as is seen in many protein−carbohydrate recognition events. This hypothesis is in agreement with high-resolution structural data for nonhydrolyzable acyl−enzyme intermediates from the picromycin TE.

Macrocyclic polyketides constitute an important class of pharmaceutical agents that include the macrolide antibiotics like erythromycin (*1*−*3*) **1** (Figure 1), antifungal agents such as pimaricin (*4, 5*) **2**, and anticancer agents, including epothilone (*6*−*8*) **3**. A common feature of all these compounds is the macrolactone functionality, which is crucial for the bioactivity and pharmaceutical utility of these molecules. Macrolactone formation is catalyzed during biosynthesis by polyketide synthase thioesterases (TEs)[1] in a two-step process (Figure 2) (*9*). First, the linear polyketide chain is loaded onto the active site serine of the TE, forming an acyl−enzyme intermediate. This is followed by nucleophilic attack of an intramolecular hydroxyl group, generating the macrocycle (*10*−*13*). When no intramolecular nucleophile is available, the acyl−enzyme intermediate is cleaved by water (*14*).

Polyketide synthase TEs have been shown to be highly specific in the chemistry they catalyze. Both acyl−enzyme intermediate formation and macrocyclization are substrate specific (*11, 13*−*16*). In vitro characterization of the loading step for different recombinant TEs with simple thioester substrates has shown that this step is substrate specific with catalytic efficiencies covering a ≥30-fold range (*14*−*17*). In vitro characterization has also shown the cyclorelease step to be highly substrate specific. For example, the 6-deoxyerythronolide B synthase (DEBS) TE appears to require a carbonyl functional group four carbons from the nucleophilic alcohol for cyclization to occur (*11, 13*). Without the carbonyl, only hydrolysis occurs. Surprisingly, the DEBS TE demonstrates broad tolerance for the ring size of the

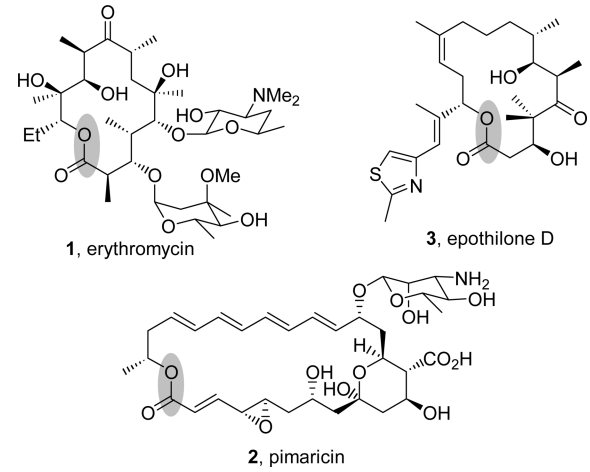

FIGURE 1: Macrocyclic polyketides, including **1**, **2**, and **3**, are formed from linear acyl chains via highly regioselective, TE-catalyzed lactone formation. The bond generated by the TE is shaded.

[†] This work was supported by Syracuse University.

* To whom correspondence should be addressed: Department of Chemistry, 1-014 Center for Science and Technology, Syracuse University, Syracuse, NY 13244-4100. Telephone: (315) 443-5803. Fax: (315) 443-4070. E-mail: cnboddy@syr.edu.

[1] Abbreviations: ACP, acyl carrier protein; CD, circular dichroism; DEBS, 6-deoxyerythronolide B synthase; FAS, fatty acid synthase; NRPS, nonribosomal peptide synthetase; PIK, pikromycin; PKS, polyketide synthase; SNAC, *N*-acetylcysteamine; TE, thioesterase.

10.1021/bi800963y CCC: $40.75
Published on Web 10/14/2008

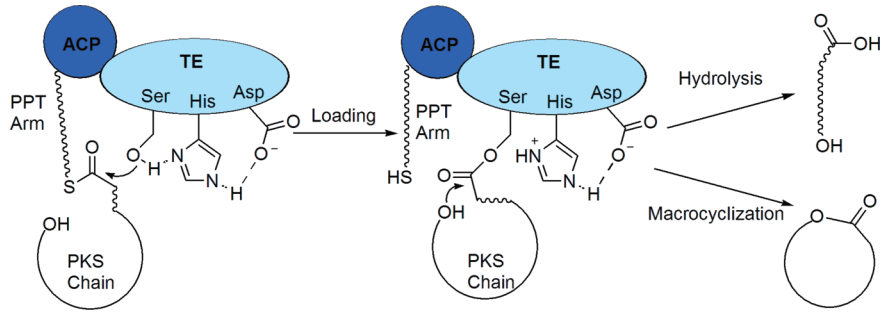

FIGURE 2: Mechanism for TE-catalyzed macrocyclization and hydrolysis of thioesters. Both the loading and macrocyclization steps are substrate selective. In the native setting, substrates are transferred from the phosphopantetheine arm of an acyl carrier protein (ACP) to the TE nucleophilic serine. Synthetic thioesters can be used to acylate the active sire serine of purified recombinant TEs. Understanding the molecular basis of substrate specificity will enable rational engineering of TE domains for loading and macrocyclizing non-native substrates.

macrocycle generated and can produce 6-, 8-, 12-, and 16-member rings in addition to the native 14-member ring system (*18*−*22*). The molecular basis for loading and macrocyclization substrate specificity is not yet well understood.

Understanding the molecular basis for substrate specificity of TEs is crucial for manipulating these enzymes to macrocyclize non-native linear polyketide chains. TE-mediated macrocyclization of non-natural linear polyketides will provide access to new macrocyclic compounds for drug discovery and development. Diverse linear chains can be produced synthetically (*23*) or enzymatically (*24*−*27*); however, known TEs are too substrate specific to effectively cyclize these diverse non-native substrates. Characterization of the molecular interactions that drive substrate specificity will enable rational engineering and focused directed evolution to modulate substrate specificity, facilitating access to these important druglike macrocyclic molecules.

The molecular basis for substrate specificity of the related nonribosomal peptide synthetase (NRPS) and fatty acid synthase (FAS) TEs (*9*) is better understood. High-resolution structural data of an NRPS TE with a noncovalently bound substrate suggest that hydrophobic interactions between the peptidyl substrate alkyl side chains and hydrophobic residues in the binding cavity play a key role in enzyme−substrate binding (*28*). High-resolution structural data of a stable covalent inhibitor−mammalian FAS TE complex show a highly hydrophobic pocket interacting strongly with the hydrophobic tail of the inhibitor (*29*). These data support hydrophobic interactions playing a key role in TE substrate recognition events.

In this study, we investigate the role of hydrogen bonding interactions in the substrate specificity of the DEBS TE. Unlike NRPS and FAS TEs, structural studies have suggested that hydrogen bonds mediate the substrate−enzyme interaction in the enzyme−substrate complex and transition state for formation of an acyl−enzyme intermediate for DEBS TE (*15, 30, 31*). Using this hypothesis, we undertook mutagenesis of 13 polar, hydrogen bonding competent residues in the binding cavity of the DEBS TE, removing the side chain hydrogen bond donors and acceptors. The specificity constant for each mutant toward hydrolysis of thioester substrates with and without hydrogen bond donors and acceptors was determined. None of the catalytically competent mutants exhibited a significant change in substrate specificity for any of the thioester substrates when compared

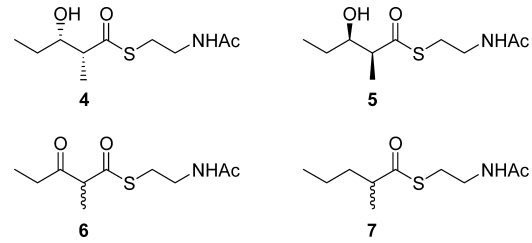

FIGURE 3: Substrates used to probe the specificity of formation of the acyl−enzyme intermediate by wild-type DEBS TE and its mutants. Substrates **4**, **5**, and **6** possess hydrogen bond acceptors; **4**, **5**, and the enol tautomer of **6** possess hydrogen bond donors, and **7** has neither hydrogen bond donors nor acceptors.

to the wild type. Our data indicate that hydrogen bonds between the substrate and enzyme do not mediate substrate specificity in the DEBS TE loading step. This result is in agreement with recent structural studies on the pikromycin TE domain with a nonhydrolyzable acyl−enzyme intermediate mimic, which suggest that nonpolar interactions dominate in mediating substrate recognition (*32, 33*). This work opens the door for rational engineering and focused directed evolution of PKS TEs (*34*) in the generation of new, needed catalysts for the production of macrocyclic products from engineered polyketide biosynthetic pathways (*24*−*27*).

MATERIALS AND METHODS

Materials. The *N*-acetylcysteamine thioester substrates **4**−**7** (Figure 3) were synthesized as previously reported (*16*). Oligonucleotide primers were purchased from Integrated DNA Technologies. Chemically competent *Escherichia coli* BL21(DE3) cells were generated according to standard protocols (*35*). Dehydrated Luria-Bertani media (Miller) was purchased from Fisher Scientific. All other reagents were purchased at >98% purity from Acros Organics, Sigma-Aldrich, or Fisher Scientific.

Acyl−*Enzyme Intermediate Modeling.* All calculations were performed using Discover version 3.0 (MSI, San Diego, CA). Chain A of the DEBS TE was extracted from Protein Data Bank entry 1kez. The acyl−enzyme intermediate was constructed using the builder module of Insight II Discover (MSI). The system was modeled using the CVFF force field. Solvent was modeled using a distance-dependent dielectric of 4*r*. The acyl−enzyme intermediate was subjected to 500 cycles of energy minimization using steepest descents, followed conjugate gradient minimization until a maximum derivative of 0.001 was achieved.

Site-Directed Mutagenesis of DEBS TE. Plasmid pRSG33 (*14*) was used as the template for site-directed mutagenesis. The following 13 mutants were generated using QuickChange site-directed mutagenesis kit (Stratagene): T76A, S80A, E84A, H141A, D169A, Y171F, N180A, E184A, T187A, H259A, T261A, M262A, and Q264A. All mutations were verified by sequencing. DNA sequencing was performed at the State University of New York Upstate Medical University DNA Core facility on an ABI 3100 DNA sequencer. Full experimental details for the construction of all 13 mutants are provided in the Supporting Information.

Expression and Purification of Wild-Type and Mutant DEBS TE. Expression vectors encoding the wild type and mutant DEBS TE were transformed into chemically competent *E. coli* BL21(DE3) cells for protein expression. Typically, 400 mL of standard Luria-Bertani medium supplemented with 50 μg/mL ampicillin was inoculated with a 0.5% (v/v) dense overnight culture of *E. coli* BL21(DE3) with the appropriate plasmid, and the culture was grown at 30 °C to an OD_{600} of 0.6. Protein expression was induced via addition of isopropyl thiogalactoside (IPTG) to a final concentration of 0.1 mM. The cultures were incubated at 30 °C with shaking at 200 rpm for 12 h.

All protein purification procedures were performed at 4 °C. The cells were harvested by centrifugation at 4000*g* and resuspended in 10 mL of lysis buffer [100 mM sodium phosphate, 300 mM NaCl, 10% (v/v) glycerol, 1 mg/mL lysozyme, 1 μg/mL pepstatin A, and 1 μg/mL leupeptin (pH 8.0)]. The cells were disrupted by sonication on ice, and cell debris was removed by centrifugation at 15000*g* and 4 °C. After addition of imidazole to a final concentration of 10 mM, the cleared lysate was incubated for 1 h with 400 μL of nickel-nitrotriacetic acid (Ni-NTA) resin (QIAGEN, Valenica, CA) and loaded onto a column. The resin was first washed with wash buffer [100 mM Tris, 300 mM NaCl, and 20 mM imidazole (pH 8.0)], and the protein was eluted with wash buffer supplemented with 250 mM imidazole. The purified protein was exchanged into dialysis buffer [100 mM Tris, 300 mM NaCl, and 30% (v/v) glycerol (pH 7.43)] and concentrated by centrifugation (Amicon 5000 MWCO). The concentrated proteins were flash-frozen in liquid nitrogen and stored at −80 °C. Protein concentrations were determined by the Bradford assay (Bio-Rad). Approximately 5 mg of purified protein was obtained per liter of cell culture with the exception of T76A, which did not provide any isolatable purified protein.

For circular dichroism and thermal denaturation experiments, protein were freshly purified following the protocol described above except that the lysis buffer did not contain glycerol and purified protein was dialyzed into buffer B [50 mM sodium phosphate (pH 7.43)] at 4 °C. Protein concentrations were determined using the Bradford assay (Bio-Rad), and each sample was diluted to 8 μM in buffer B immediately before analysis.

Kinetic Analysis of Wild-Type and Mutant DEBS TE. The TE-catalyzed hydrolyses of thioester substrates **4**, **5**, **6**, and **7** were monitored by observation of the formation of 5-thio-2-nitrobenzoate by reaction of released *N*-acetylcysteamine with 5,5′-dithio-2-nitrobenzoic acid (DTNB), as previously described (*16*). A typical kinetic assay mixture consists of 5 μM wild-type or mutant DEBS TE protein, 50 mM phosphate buffer (pH 7.43), a 4% (v/v) saturated solution of DTNB in 50 mM phosphate buffer (pH 7.43), 1 mM substrate (100 or 10 mM stock solutions in DMSO), and 10% (v/v) DMSO in a total volume of 100 μL. The formation of free thiol was quantified by measuring the absorption at 412 nm using a GENESYS 20 spectrophotometer (Thermo Electron Corp., Madison, WI). The reactions were monitored for 12 min at room temperature, and data points were collected every 2 min. Initial velocities were determined by linear regression analysis of the data. All steady state kinetic assays were performed with five different concentrations (0.2, 0.4, 1.0, 2.0, and 4.0 mM) of the substrate in duplicate. The measured reaction rates were corrected for background chemical hydrolysis in the absence of protein. The kinetic parameter k_{cat}/K_M was calculated from the slope of v versus [S] (see the Supporting Information). Because of apparent variation in specific activity among protein preparations, a single protein preparation was used for determination of the specificity constant for substrates **4**−**7** (*14*−*16*).

Circular Dichroism Spectra. Circular dichroism spectra were collected on a model 202 spectropolarimeter (Aviv Biomedical). All data were recorded from 196 to 260 nm at 10 °C in a 1 mm path length cell. The spectral bandwidth was 1.0 nm, the step size 1 nm, and the averaging time 10 s. Each spectrum was recorded in duplicate.

Thermal Denaturation. Temperature-induced unfolding of DEBS TE was monitored at 220 nm in a 1 mm path length cell. The samples were heated from 10 to 55 °C in increments of 1 °C. The heating rate was 2 °C/min and the averaging time 30 s, and a 30 s thermal equilibration time was established at each newly set temperature. Each experiment was performed in duplicate. The thermal denaturation curves were analyzed by a nonlinear least-squares fit according to eq 1 (*36, 37*).

$$Y = \frac{y_n + m_n T + (y_d + m_d T)\exp[\Delta H_m/R(1/T_m - 1/T)]}{1 + \exp[\Delta H_m/R(1/T_m - 1/T)]} \quad (1)$$

where Y is the measured ellipticity, ΔH_m is the enthalpy at the unfolding transition, T_m is the melting temperature, T is the temperature, R is the universal gas constant, m_n is the slope of the pretransition baseline, y_n is the intercept of the pretransition baseline, m_d is the slope of the post-transition baseline, and y_d is the intercept of the post-transition baseline.

RESULTS

The thioesterase domain from the 6-deoxyerythronolide B biosynthetic pathway (DEBS TE) was identified as the optimal thioesterase for the study of substrate specificity. Recombinant DEBS TE has been kinetically characterized in vitro, and crystallographic analysis has generated multiple high-resolution structures of the enzyme (*30, 31, 33*). The native product from DEBS TE-catalyzed macrocyclization, 6-deoxyerythronolide, has been computationally docked into the crystollographically derived DEBS TE binding cavity (*30*). Analysis of the docked structure showed a number of key hydrogen bond interactions between the alcohol rich substrate and the hydrophilic residues that line the binding cavity (Figure 4). In particular, the alcohol at C3 was proposed to hydrogen bond to the side chain of N180, the alcohol at C5 was proposed to interact with the side chains

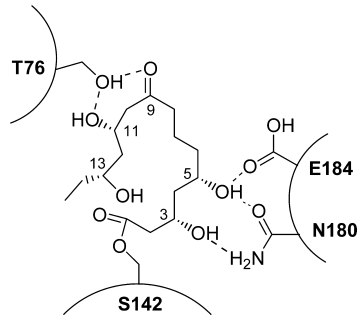

FIGURE 4: Model depicting proposed hydrogen bonding interactions between the DEBS TE and 6-deoxyerythronolide. Only 6-deoxyerythronolide functional groups involved in hydrogen bonding with the TE binding cavity are depicted. Hydrogen bonding was proposed as the key mechanism driving substrate specificity in TE-catalyzed hydrolysis and macrocyclization.

of both N180 and E184, and the C9 keto and C11 alcohol were both proposed to interact with the side chain alcohol of T76.

On the basis of this model, it has been proposed that hydrogen bonding between the substrate and N180 and E184 drives substrate specificity during rate-limiting acyl−enzyme intermediate formation. Substantial evidence supports acylation of the active site serine being the rate-limiting step in PKS TE-mediated hydrolysis. First, PKS TEs are homolgous to the well-characterized animal FAS TEs, which have been shown to undergo rate-limiting acylation (*38, 39*). Second, substrates with better leaving groups undergo faster hydrolysis, suggesting either acylation or leaving group release is rate-limiting (*14, 17*). Third, we have been unable to detect pre-steady state burst kinetics for PKS TEs, indicating that leaving group release, hydrolysis, or product release is not rate-determining. While there is a single literature example of a wild-type TE domain exhibiting burst kinetics, this TE possesses a wildly divergent catalytic nucleophile sequence, which may explain its unusual reactivity (*40*). Finally, we have also been unable to detect acylated TE domains by mass spectrometry experiments, indicating that they do not accumulate appreciably and that their formation is rate-limiting. These results strongly suggest that acylation of the active site serine is the rate-limiting step in TE-mediated hydrolysis and that kinetic data will provide characterization of events leading up to and including this step.

Because the hydrogen bonding interactions should be present in and stabilize the enzyme−substrate complex and the transition state for the acyl−enzyme intermediate, modulations of these stabilizing interactions should affect the hydrolytic rate constants. For example, loss of these stabilizing interactions should decrease k_{cat}, increase K_M, and decrease k_{cat}/K_M. Literature data supporting hydrogen bond-mediated substrate specificity during acyl−enzyme intermediate formation include in vitro characterization of the hydrolysis rates of the wild-type DEBS TE with enantiomeric substrates **4** and **5** and mutants of the homologue TE from the pikromycin biosynthetic pathway (PIK TE) with substrates **4**, **5**, and **6**. Recombinant purified DEBS TE hydrolyzes substrate **4** with a specificity constant 4−15-fold greater than that of substrate **5** (*14, 15, 30*). These data support specific hydrogen bonding interactions between the C3 hydroxyl group of the substrate and the binding cavity, which drive recognition during rate-determining acyl−enzyme intermediate formation (*14, 17*). Inversion of the C3 hydroxyl group is proposed to disrupt the hydrogen bonding interactions, decreasing the specificity constant for acyl−enzyme intermediate formation. Mutation of both E187 and R191 in PIKS TE, residues that correspond to DEBS TE N180 and E184, respectively, reverses selectivity with substrate **5** being preferred over **4** when compared to the wild-type PIK TE (*15*). These data suggest that the side chains of residues corresponding to DEBS TE N180 and E184 may have key specific interactions, likely hydrogen bonding interactions, with the C3 hydroxyl group of the substrate during acyl−enzyme intermediate formation.

To unambiguously probe the role of hydrogen bond interactions in mediating substrate recognition and acyl−enzyme intermediate formation in the DEBS TE, we set out to compare hydrolytic rates for substrates with (**4**, **5**, and **6**) and without (**7**) hydrogen bond donors and acceptors at C3 with a panel of DEBS TE mutants in which binding cavity residues were mutated to remove side chains containing hydrogen bond donors and acceptors. Because hydrogen bonding interactions will stabilize both the enzyme−substrate complex and the transition state, we hypothesized that k_{cat} will decrease, K_M will increase, and k_{cat}/K_M will decrease for hydrolysis of substrates containing hydrogen bond donors or acceptors if the hydrogen-bonding partner in the binding cavity is removed by mutagenesis. Substrates that do not contain hydrogen bond donors or acceptors may see a small increase in k_{cat}, a decrease in K_M, and a corresponding increase in k_{cat}/K_M for hydrolysis upon removal of hydrogen bonding competent residues in the binding cavity due to the increase in hydrophobicity. Thus, comparison of the relative hydrolytic rate for the wild-type and mutant TE with substrates that contain hydrogen bond donors and acceptors and those that do not will provide a means for assessing the role of the residue in substrate specificity, while controlling for nonspecific loss of enzymatic activity due to general perturbation of the fold and active site cavity.

To identify appropriate binding cavity residues to mutate, a model of a simple acyl−enzyme intermediate was generated. The A chain from the 2.8 Å resolution DEBS TE crystal structure (*30*) was retrieved from the Protein Data Bank. A model of the acyl−enzyme intermediate was constructed via acylation of the active site serine side chain, S148, with a (2*R*,3*S*)-3-hydroxy-2-methylpentanoyl group. The position of the protein was held constant, and energy minimization was performed to generate an acyl−enzyme intermediate model. No specific hydrogen bonding interactions between protein and substrate were identified from this model. Unlike 6-deoxyerythronolide B, which can be docked into the binding cavity in one preferred orientation, simple acyl chains can be docked in a myriad of different configurations. The computational flexibility of the short acyl−enzyme intermediate suggested that the substrate could interact with a number of different residues in the active site and thus that binding of the simple acyl chain substrates may not be representative of the full-length native substrate.

Examination of the literature shows that simple acyl chain substrates behave like longer chain acyl substrates. For example, DEBS TE hydrolyzes the diketide **4** preferentially over **5** and shows identical selectivity for the absolute configuration of the alcohol (*S*) and methyl group (*R*) in the hydrolysis of triketide and heptaketide substrates. This

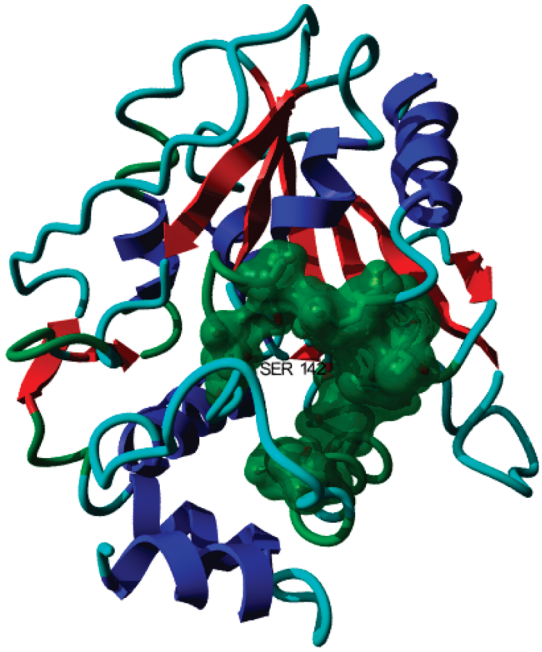

FIGURE 5: Structure of the DEBS TE showing the location of polar residues that were targeted for mutagenesis.

conserved substrate specificity suggests that the binding mode for the simple substrates is reflective of larger, more native substrates. Comparison of kinetic data for hydrolysis of **4** versus macrocyclization of a long chain hexaketide substrate by DEBS TE shows their specificity constants to be within a factor of 2.5 (*13, 14*). Analysis of structural data for nonhydrolyzable acyl−enzyme intermediates of PIK TE shows that tri- and pentaketide substrates adopt highly similar conformations in the enzyme (*32, 33*). These diverse data further support the validity of using simplified substrates to probe the binding mode. Additionally, the crystallographic data for the PIK TE show well-defined electron density maps for the small triketide substrates, indicating that they are not mobile in the binding cavity (*32*). These data support low mobility of small substrates in PKS TE binding cavities and a similar binding mode between small substrates and larger, more native substrates. On the basis of these literature results, we concluded that the use of substrates **4**−**7** would provide meaningful data that could be extrapolated to aid in predicting substrate tolerance of larger more native substrates in DEBS TE.

To ensure adequate sampling of the potential hydrogen bonding competent residues with which the acyl chain could interact, all polar amino acids lining the binding cavity and within 8 Å of the acyl chain from the model were selected for mutagenesis (Figure 5); T76, S80, E84, H141, D169, Y171, N180, E184, T187, H259, T261, M262, and Q264 residues were identified. D169 and H259, which are part of the catalytic triad, were included. Mutation of these residues to alanine is expected to produce inactive proteins; thus, these two residues represent negative controls, and kinetic characterization of these mutants will confirm the roles of H259 as the general base in the reaction and D169 as the general acid (*30, 41*). These 13 residues were individually mutated to alanine in all cases except for Y171, which was mutated to phenylalanine, generating a library of 13 single DEBS TE mutants.

Steady State Kinetic Analysis of Wild-Type and Mutant DEBS TEs. The Michaelis−Menten specificity constants (k_{cat}/K_M) for wild-type and mutant TEs were measured for substrates **4**−**7**. The results are summarized in Table 1. Determination of the Michaelis constant (K_M) and the turnover number (k_{cat}) would provide more detailed data for testing our hypothesis. Following the Michaelis−Menten mechanism, K_M provides information about the stability of the enzyme−substrate complex relative to the free substrate and enzyme and k_{cat} provides information about the stability of the transition state relative to the enzyme−substrate complex. These data would enable the useful deconvolution of hydrogen bond stabilization of the substrate−enzyme complex versus the transition state. However, the K_M values determined for the hydrolysis of simple substrates, like **4**−**7**, by bacterial polyketide synthase TEs have been very high, typically 5−30 mM (*14, 15*). This concentration range is above the solubility range of **4**−**7** in the assay buffer; thus, accurate determination of k_{cat} and K_M is not possible. Because the kinetic data are collected at concentrations well below the value of K_M and thus K_s, the value of k_{cat}/K_M can be interpreted as reflecting the Gibbs free energy difference between the transition state for acylation and the free enzyme and substrate. Thus, our data will not be able to detect interactions that stabilize or destabilize the enzyme−substrate complex without influencing the transition state (*42*).

A number of different specificity constants were determined for the wild-type DEBS TE with substrates **4**, **5**, and **6**. For example, the specificity constant for hydrolysis of **4** ranges from 0.60 to $5.3 \pm 1.2\ M^{-1}\ s^{-1}$ in the literature (*14, 15*). This difference has been attributed to variations in the preparation of the recombinant purified protein (*15*). Because of the substantial variation in specificity constants obtained for the same TE with the same substrate, we were concerned about the validity of conclusions drawn from comparison of specificity constants. To address this concern, we examined the reproducibility of the magnitude of the specificity constant for substrates **5** and **6** normalized to the magnitude of the specificity constant of **4**. Our preparations reproducibly gave normalized specificity constants of 0.22 ± 0.03 and 1.4 ± 0.2 for **5** and **6**, respectively (note that kinetic analysis for all substrates was performed using the same preparation of protein). Normalization of literature specificity constants also produced very similar values for compounds **5** and **6**, 0.23 ± 0.17 and 1.7 ± 0.5, respectively, even in cases where the absolute values of the specificity constants differed by more than 10-fold (*14, 15*). On the basis of these observations, specificity constants that have been normalized to the magnitude of one of the four substrates are expected to provide reliable and reproducible results.

Normalized specificity constants obtained from the ratio of hydrogen bond donor- and acceptor-containing substrates, **4**−**6**, to **7**, the substrate without a hydrogen bond donor or acceptor at C3, were selected as the optimal ratios for our analysis. These ratios were expected to maximize the change in normalized specificity constants based on our hypothesis. If hydrogen bonding interactions are stabilizing the transition state, the specificity constant for the wild-type enzyme with a hydrogen bond donor- or acceptor-containing substrate is expected to be maximized relative to the specificity constant for a similar substrate without the hydrogen bond donor or acceptor. This is due to the added stabilization of the

Table 1: Absolute and Normalized Michaelis−Menten Specificity Constants for Hydrolysis of **1**−**4** with Wild-Type and Mutant DEBS TEs

	k_{cat}/K_M (M^{-1} s^{-1})						
	4	**5**	**6**	**7**	**4/7**	**5/7**	**6/7**
wild type	0.50 ± 0.03	0.111 ± 0.006	0.70 ± 0.07	0.17 ± 0.01	2.9 ± 0.3	0.65 ± 0.07	4.1 ± 0.7
S80A	1.40 ± 0.06	0.35 ± 0.01	2.85 ± 0.08	0.51 ± 0.01	2.9 ± 0.3	0.67 ± 0.03	5.6 ± 0.7
N180A	0.28 ± 0.01	0.123 ± 0.008	0.52 ± 0.04	0.14 ± 0.01	2.0 ± 0.2	0.88 ± 0.12	3.7 ± 0.5
E184A	0.90 ± 0.03	0.149 ± 0.006	1.90 ± 0.04	0.30 ± 0.01	3.0 ± 0.2	0.50 ± 0.04	6.3 ± 0.3
T261A	0.60 ± 0.01	0.099 ± 0.008	1.00 ± 0.05	0.16 ± 0.01	3.8 ± 0.3	0.62 ± 0.09	6.3 ± 0.7
Q264A	0.83 ± 0.03	0.151 ± 0.008	2.00 ± 0.07	0.25 ± 0.01	3.3 ± 0.3	0.60 ± 0.06	8.0 ± 0.6

transition state by the hydrogen bonding interaction. In a mutant where the hydrogen bonding interaction has been eliminated, the ratio of specificity constants is expected to be at a minimum. The specificity constant for the hydrogen bond donor- or acceptor-containing substrate should decrease relative to the wild-type value due to a loss of the hydrogen bond stabilizing the transition state. In addition, the transition state for hydrolysis of **7**, which does not possess a hydrogen bond donor or acceptor, is expected to be stabilized in the mutant. This stabilization is due to the stronger hydrophobic interaction between the substrate and the binding cavity as well as the removal of the destabilizing effect of an unpaired hydrogen bond donor or acceptor in the binding cavity. In this case, the normalized specificity constant should be minimized. On the basis of this analysis, loss of a transition state-stabilizing hydrogen bonding interaction between the substrate and the enzyme should lead to a noticeable decrease in the ratio of specificity constants for hydrolysis of **4**, **5**, or **6** versus **7**.

Kinetic characterization of the recombinant expressed mutants showed that five of the 12 mutations were active (S80A, N180A, E184A, T261A, and Q264A) and seven were inactive (E84A, H141A, D169A, Y171F, T187A, H259A, and M262A). The five active mutant TEs exhibited very similar substrate specificity for hydrolysis of **4**−**7** when compared to the wild-type TE. Examination of the normalized specificity constant **4/7** and **5/7** ratios shows that the majority of these values are identical within error to the wild-type data. Key exceptions are the N180A and E184A mutants. The **4/7** data for N180A are 30% lower than the wild-type data. This indicates that relative to that of the wild type the specificity constant for hydrolysis of **4** decreases more than the specificity constant for hydrolysis of **7**, supporting a role for the N180 side chain in transition state stabilization. Because substrate **7** differs from **4** in the lack of a hydroxyl group at C3, the decrease in the relative magnitude of the specificity constant between the wild type and mutant supports a hydrogen bonding interaction between N180 side chain and C3 hydroxyl group of **4**. Similarly, the **5/7** data for the E184A mutant show a 20% decrease as compared to that of the wild type, indicating that the side chain of E184 is likely interacting with the C3 hydroxyl group of **5**. The relatively small change in specificity between the wild type and the N180A and E184A mutants suggests that this hydrogen bonding interaction plays at best a minor role in controlling substrate specificity (see Discussion).

Some of the **4/7** and **5/7** normalized specificity constants show an increase over that of the wild type. This is seen for T261A **4/7** and N180A **5/7** data. The change indicates that the specificity constant for substrate **5** is increasing relative to that of **7** in the mutant versus the wild-type enzymes. This data cannot be rationalized by the loss of hydrogen bonding interaction between the substrate and binding cavity and thus represent the variability in substrate specificity due to nonspecific perturbation of the binding cavity in the mutants. The magnitude of the increase over that of the wild type is between 30 and 35%. Changes in the normalized specificity constants smaller in magnitude than this thus may not reflect actual mechanism specific perturbations such as loss of hydrogen bonding interactions.

Examination of the **6/7** normalized specificity constants shows some change in substrate specificity between the mutant and the wild-type enzyme. The data for the N180A mutant are identical within error to those for the wild-type enzyme. The data for the S80A, E184A, T261A, and Q264A mutants show an increase in relative specificity constants versus the wild type. S80A, E184A, and T261A show a 37−54% increase in relative magnitude, whereas Q264A shows a 95% increase. The increase in normalized specificity constant cannot be rationalized by the loss of hydrogen bonding interaction between the substrate and binding cavity.

Thermal Denaturation of Wild-Type and Mutant DEBS TEs. Steady state kinetic analysis showed that seven mutants were catalytically inactive (E84A, H141A, D169A, Y171F, T187A, H259A, and M262A). Two hypotheses can account for the loss of activity. The mutated residue may play a critical role in catalysis or substrate recognition; thus, when the protein is mutated, enzymatic activity is abolished or greatly reduced. Alternatively, the residue may play an important role in the kinetics or thermodynamics of folding, and mutation to alanine leads to incorrectly folded or unstructured proteins. To examine these two hypotheses, circular dichroism spectroscopy was used to assay the extent of secondary structural elements in the mutants and to determine the relative stabilities of the protein tertiary structure (*43*).

Circular dichroism spectroscopy and thermal denaturation were performed on the wild type and mutant DEBS TEs. Figure 6 shows the thermal denaturation curve of the wild type and three representative mutants (all CD spectra and thermal denaturation curves can be found in the Supporting Information). The melting temperatures of the wild type and folded mutants are reported in Table 2.

The circular dichroism spectrum of the wild-type TE exhibits double negative maxima at 208 and 220 nm, which are typical for a fold with substantial α-helical character (*43*). The thermal denaturation curve of the wild type can be fitted into a cooperative two-state model for unfolding, generating a melting temperature (T_m) of 305.5 ± 0.3 K. The five catalytically active mutants (S80A, N180A, E184A, T261A, and Q264A) all exhibit double maxima at 208 and 220 nm in their CD spectra and comparable melting temperatures (T_m). The majority of the catalytically inactive mutants (E84A, H141A, H259A, and M262A) do not display the

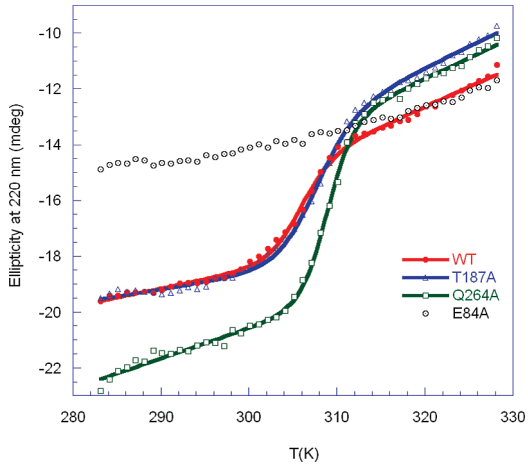

FIGURE 6: Thermal denaturation curve of the wild-type DEBS TE and representative mutants.

Table 2: Melting Temperatures of the Wild Type and Folded Mutants

	T_m (K)
wild type	305.5 ± 0.3
S80A	305.4 ± 0.2
N180A	306.0 ± 0.2
E184A	305.8 ± 0.5
T261A	298.9 ± 0.6
Q264A	308.8 ± 0.2
D169A	304.4 ± 0.2
Y171F	305.7 ± 0.2
T187A	307.5 ± 0.3

double maxima at 208 and 220 nm and do not undergo a cooperative two-state thermal denaturation, indicating little α-helical content and a lack of defined tertiary structure. The remaining catalytically inactive mutants (D169A, Y171F, and T187A) underwent thermal denaturation, and the data could be fit to a two-state cooperative unfolding model, providing T_m values similar to that of the wild-type TE.

DISCUSSION

To study the role of hydrogen bonding in substrate specificity for formation of the acyl−enzyme intermediate by bacterial polyketide synthase TE domains, we constructed a number of TE mutants and determined their substrate specificities. The principle literature model rationalizing substrate specificity for the DEBS TE domain postulates key hydrogen bonding interactions between the substrate and the side chains of residues in the enzyme binding cavity (*30*). To test this hypothesis, 13 residues with hydrogen bond donors and acceptors within the DEBS TE binding cavity were mutated to either alanine or phenylalanine. Four substrates, three with hydrogen bonding functional groups and one without, were used to assay changes in substrate specificity with the TE mutants. No significant change in substrate specificity was observed with any of the active mutants for the four substrates, indicating that hydrogen bonding interactions do not drive substrate specificity.

To identify residues for site-directed mutagenesis, an in silico model of the acyl−enzyme intermediate was generated. This model was used to identify polar side chains in the binding cavity that came into close contact with the acyl group of the acyl−enzyme intermediate. Thirteen polar residues were identified using this approach. Alignment of the DEBS TE with 10 other PKS TE domains (see the Supporting Information) showed that seven of the 13 residues were highly conserved (E84, H141, D169, Y171, H259, T261, and M262). Two residues (T76 and S80) were partially conserved, occurring as either a threonine or proline and a serine or a glycine, respectively. The four remaining residues (N180, E184, T187, and Q264) were highly variable.

Kinetic analysis of the mutants showed that five were catalytically active (S80A, N180A, E184A, T261A, and Q264A). Three of the catalytically active mutants contained mutations of highly variable residues (N180A, E184A, and Q264A). The mutant of the partially conserved S80 was also active. Mutations of the highly conserved residues (E84, H141, Y171, and M262) lead to catalytically inactive proteins. Mutation of the highly variable T187 provided a catalytically inactive protein. The lack of activity for the T187A mutant is surprising since the TE domain from the pikromycin and niddamycin biosynthetic pathways (*44, 45*), which are both >39% identical to DEBS TE, can accommodate leucine and glycine, respectively, at this position. As expected, mutation of the highly conserved catalytic triad residues (D169 and H259) resulted in catalytically inactive mutants, confirming the role of these residues in catalysis. Mutation of the partially conserved T76 provided a construct that did not provide appreciable amounts of soluble protein.

A residue of particular interest is T261. Unlike all other highly conserved residues mutated in this study, mutation of T261 to alanine leads to a catalytically active protein. T261 is part of an exposed surface loop in the excised, recombinant TE and does not show any contacts to other residues (*30, 31*). It is close to the proposed acyl carrier protein (ACP) binding site and at the exposed opening of the substrate cavity (*30*). We thus propose that T261 is highly conserved because it aids in stabilizing the entry of the acylated phosphopantetheine arm of the ACP into the TE binding pocket during acyl−enzyme intermediate formation in the native polyketide synthase system. Recent evidence suggests that the acyl−enzyme intermediate attached to the phosphopantetheine arm of bacterial PKS ACP domains is not exposed to solvent (*46*), but rather buried in the ACP domain, similar to the *E. coli* FAS ACP structure (*47*). An interaction between the side chain of T261 may play a role in extracting the acyl−phosphopantetheine arm from a buried conformation to an extended conformation like the conformation seen in the *Saccharomyces cerevisiae* FAS ACP domain (*48*). Thus, T261 may play a critical role in ensuring transfer of the completed acyl chain from the ACP domain to the TE domain in the context of the native polyketide synthase system, ensuring that it is highly conserved. Because the excised recombinant TE domains do not interact with the ACP domains in our in vitro characterization and the substrates contain highly truncated analogues of the phosphopantetheine arm, T261 will not have a binding partner with which to interact. Thus, the T261A mutant is not expected to exhibit a loss of activity. This hypothesis can be tested via an examination of the role of T261 in the in cis or in trans interaction of ACP domains with TEs (*49*).

The kinetic data provide information about the enzymatic steps leading up to acyclation of the active site serine. We have demonstrated that acylation is rate-determining for TE-catalyzed hydrolysis of simple alkyl thioester substrates. Specificity constants therefore provide information about the relative stability of the transition states for acylation of S142.

Comparison of specificity constants for the different substrates and mutants provides information about changes in the relative stability of the transition states, helping to identify molecular interactions that drive substrate specificity for TE acylation. It should be noted that the kinetic data cannot provide information about the molecular interactions that govern hydrolysis or macrocyclization because these chemistries occur after active site acylation, and if the rate-determining step for TE-catalyzed chemistry changes, new interactions may drive substrate specificity.

Examination of the specificity of the catalytically active mutants for substrates **4**−**7** showed that none of the mutations significantly changed the substrate specificity. Small variations of 20−40% in the relative magnitudes of the specificity constants were seen for substrates **4**, **5**, and **6** with all the active mutants. If hydrogen bonding interactions are present between the substrate and side chain of the mutated residue in the transition state of the reaction, then large changes in the relative magnitude of the specificity constants would have been seen. This is especially the case for the ratio of specificity constants of substrates **4** with **7** and **5** with **7**. If the side chain was hydrogen bonding to the 3-hydroxyl group of **4** or **5** in the transition state, then the magnitude of the specificity constant relative to **7**, which does not have the 3-hydroxyl group, should decrease significantly for the mutant. This is because substrates **4** and **5** would lose a critical stabilizing interaction in the transition state as the side chain is deleted. Deletion of the side chain does not affect substrate **7** because there is no interaction in the transition state of the wild type or mutant. Combined substrate and mutagenesis effects have been used to demonstrate the importance of hydrogen bonding interactions in the 4-hydroxybenzoyl coenzyme A thioesterase (*50*). With this thioesterase, mutations lead to a 15-fold decrease in relative specificity constants. Large (≥10-fold) changes in substrate specificity have also been observed in RNases, DNA topoisomerases, uracil DNA glycosylases, and protein tyrosine phosphates, confirming the presence of hydrogen bonding interactions between specific residues and the substrates in the transition states (*51*). The small magnitudes of the changes in substrate specificity of the DEBS TE mutants for substrates **4**−**7** indicate that there are no hydrogen bonding interactions between residues S80, N180, E184, T261, and Q264 and the substrate in the transition state. These experimental data disagree with the hypothesis that hydrogen bonding interactions drive substrate specificity for substrate loading in PKS TE domains (*30*).

Circular dichroism spectroscopy and thermal denaturation showed that the wild-type TE and eight mutants (S80A, D169A, Y171F, N180A, E184A, T187A, T261A, and Q264A) were folded. Analysis of the CD spectrum for the wild type indicated substantial α-helical content, which is in agreement with the known high-resolution structure of the DEBS TE. Thermal denaturation showed that the wild-type DEBS TE underwent cooperative two-state unfolding with a melting temperature of 305.5 ± 0.3 K (32.4 ± 0.3 °C). The low melting temperature indicates that kinetic characterization of PKS TE domains should be carried out at or below room temperature. The majority of in vitro characterization of PKS TE domains have been performed at 30 °C (*14, 15*). Our data suggest that the TE domains may be partially unfolded at this temperature. Partial unfolding of the TE domain during kinetic characterization may provide a mechanism for the variation seen in the literature for the specificity constants with substrates **4** and **5**. All the catalytically active mutants were shown to be well-folded. Their CD spectra showed significant α-helical content and thermal denaturation melting temperatures comparable to that of the wild-type TE.

The three mutants (D169A, Y171F, and T187A) showed no catalytic activity but were determined to be folded by CD spectroscopy. D169 is postulated to be the general acid in the TE catalytic triad (*30*). The lack of hydrolytic activity in the folded D169A mutant experimentally supports this role of the side chain carboxylate in the catalytic mechanism. The Y171F mutation is likely inactive as it may cause the overall structure of the TE to adopt a catalytically inactive conformation. Crystallographic analysis of the DEBS TE has identified a second form of the enzyme (Protein Data Bank entry 1mo2) in which the catalytic base, H259, is displaced from the binding pocket (*31*). This form is predicted to be catalytically inactive. It, however, has an overall fold very similar to that of the catalytically active form and thus is expected to provide comparable CD spectra and thermal denaturation data (Figure 8). The second form occurs through the displacement of the two loops containing residues 233−244 and 256−265. A key interaction stabilizing the loop containing residues 233−244 in the catalytically active form is a hydrogen bond between the phenol of Y171 and the backbone NH group of K243 (*30, 31*). In the Y171F mutant, we postulate that this hydrogen bonding interaction is removed, destabilizing the loop containing residues 233−244 and leading to formation of the second, catalytically inactive form of the DEBS TE. It is surprising that the T187A mutant is catalytically inactive and well-folded. Alignment shows that T187 is highly variable, with both hydrophobic and hydrophilic residues being accommodated at this position. It is unlikely that T187 is playing a key mechanistic role in catalysis. On the basis of structural data, T187 appears hydrogen bonded principally to it own NH group. Loss of this hydrogen bonding interaction is unlikely to drive the structure into the second catalytically inactive form of the enzyme. It is possible that T187A plays a key role during the folding process in directing the overall fold to the catalytically active form and that mutation to alanine disrupts this folding process leading to the second form.

Our data show that alanine mutants of polar, highly conserved residues in the binding cavity cannot fold into stable tertiary structures. A particularly unique aspect of TE domains when compared to α/β-serine hydrolases is the presence of a channel through the protein (*30*). The linear substrate is proposed to enter one side of the channel and exit as the macrocycle from the other side of the channel. We thus propose that the highly conserved residues present in the binding cavity, including E84, H141, and M262, are required to solvate the channel and prevent its collapse (*31*). With the mutation to alanine, the channel is substantially destabilized, leading to an unstable tertiary structure and misfolding.

In summary, we have demonstrated via kinetic characterization of bacterial PKS TE mutants that hydrogen bonding interactions between the substrate and enzyme do not drive substrate specificity for acyl−enzyme intermediate formation, which has been proposed in the literature. This conclusion

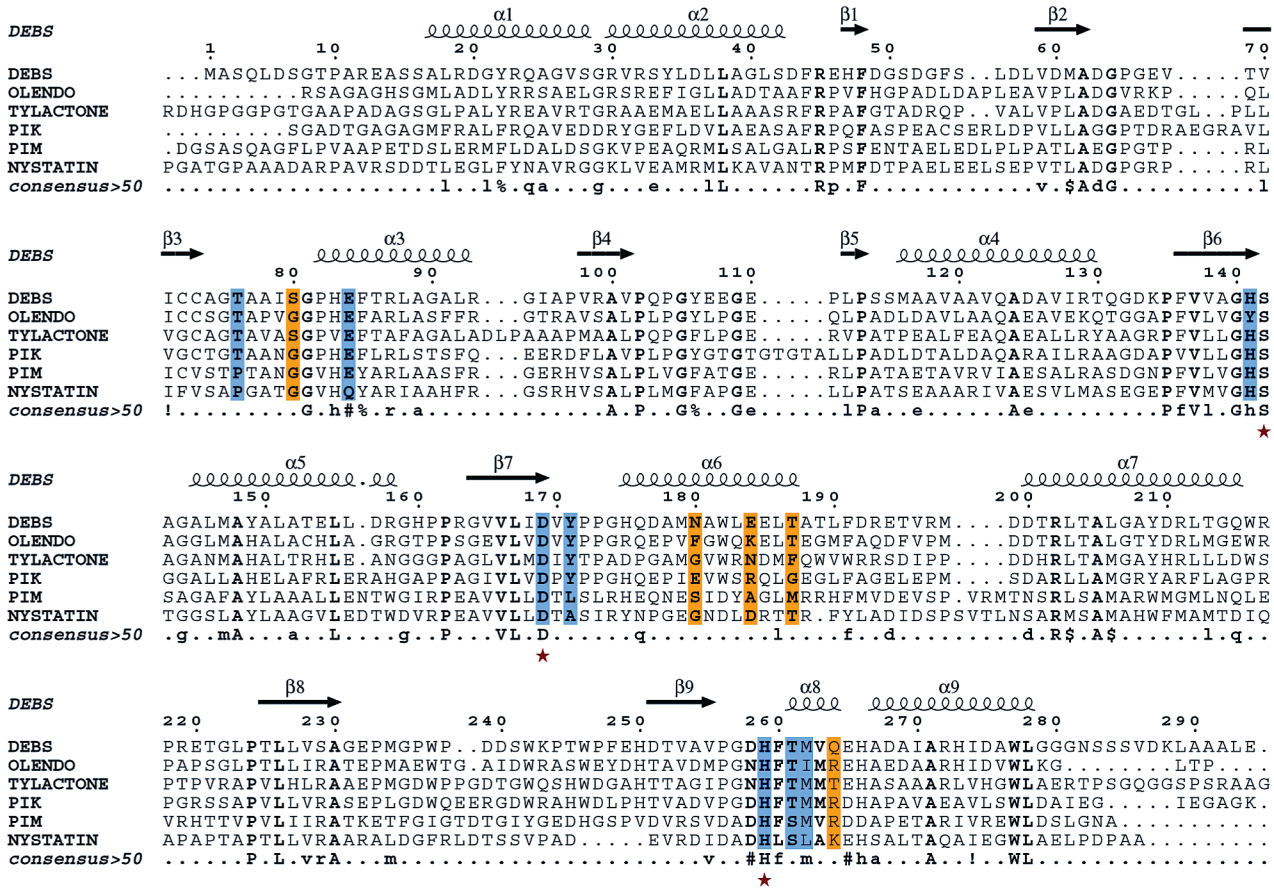

FIGURE 7: Sequence alignment of bacterial polyketide synthase TE domains. Alignment was performed using clustalX1.83. Mutated conserved residues are colored purple, and mutated nonconserved residues are colored yellow. Catalytic triad residues are labeled with asterisks. Secondary structural elements from the DEBS TE are shown above the sequence. OLEANDO is the TE from the oleandomycin biosynthetic pathway. TYLACTONE is the TE from the tylactone biosynthetic pathway. PIK is the PIK TE. PIM is the TE from the pimaricin biosynthetic pathway. NYSTATIN is the TE from the nystatin biosynthetic pathway.

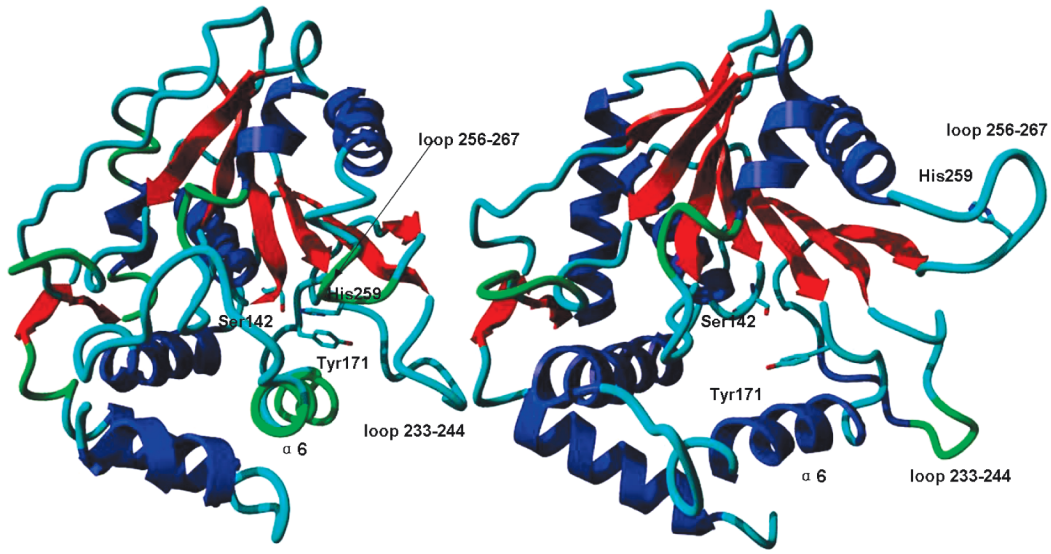

FIGURE 8: Two different high-resolution structures of the DEBS TE have been identified. The native structure on the left is catalytically active, whereas the alternative structure on the right is catalytically inactive due to the displacement of the catalytic base, H259 from the binding pocket. Mutation of Y171 to alanine leads to the Y171A mutant adopting the folded but catalytically inactive structure on the right.

is in agreement with recent high-resolution structural data of nonhydrolyzable acyl−enzyme intermediates of the homologous PIK TE (*32, 33*). This structural data show a lack of specific, direct contacts between the substrate and enzyme.

On the basis of these results, a model dominated by hydrophobic interactions between the binding cavity and the substrate can be proposed. Using Ligand Explorer (http://www.kukool.com/ligand/help/), the structure of the pentaketide affinity labeled PIK TE (Protein Data Bank entry 2hfj)

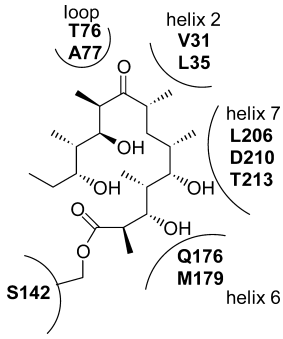

FIGURE 9: Hydrophobic model for substrate recognition in DEBS TE. No specific, direct hydrogen bonding contacts between the binding cavity and substrate acyl chain are generated. Hydrophobic packing of the acyl chain in the binding pocket drives recognition.

exhibits strong hydrophobic interactions (1.9−4.1 Å in distance) between the pentaketide and protein. The residues involved in the hydrophobic interactions can be mapped onto the primary structure of the DEBS TE, identifying nine residues (V31, L35, T76, A77, Q176, M179, L206, D210, and T213). Assuming that the native DEBS TE acyl−enzyme intermediate folds into the active site in a manner similar to that of the PIK TE acyl−enzyme intermediate, a partial model for hydrophobic interactions that can govern substrate specificity can be constructed (Figure 9). Because the native DEBS TE acyl chain is a heptaketide, the pentaketide affinity label used in the PIK TE structural study provides no data to support the interactions driving recognition of the remaining two ketide units. Examination of the two triketide affinity labeled PIK TE high-resolution structures (Protein Data Bank entries 2h7x and 2h7y) supports the proposed model, showing as expected the triketide label interacting with hydrophobic residues form helix 6 and helix 7.

A rigorous computational study aimed at determining the binding mode of the native substrate and **4**−**7** with DEBS TE will provide complementary insights into the specific molecular interactions between the binding cavity and substrates. Because the native substrate is large in size and the binding cavity for the substrate is buried in the interior of the TE, docking studies will require that the docking site and many of the surrounding structural elements be highly flexible to accommodate induced fit binding. These computational studies are currently underway and are expected to provide data further clarifying the binding mode for substrates in DEBS TE and the validity of using simple substrates like **4**−**7** in probing the binding mode.

Hydrophobic interactions between highly oxygenated substrates and proteins are not unprecedented mediators of substrate specificty. Like polyketides, carbohydrates have numerous alcohols rendering them obvious partners for hydrogen bonding interactions with the protein backbone and side chains (*52*). However, a substantial portion of specificity for carbohydrate−protein interactions involves hydrophobic packing with protein side chains. Mutagenesis of hydrophobic residues involved in van der Waals interactions has led to substantial changes in carbohydrate−protein interactions (*53*). Mutagenesis of hydrophobic residues in PKS TE is thus expected to aid in modifying substrate specificities of these TEs. Because of the mobility of carbohydrate substrates in their binding pockets, rational approaches to modulating substrate specificity have not been successful while directed evolution approaches have been (*54, 55*). Once experimentally confirmed, this hydrophobic model will facilitate engineering of TEs for loading and macrocyclizing nonnative substrates (*34*).

ACKNOWLEDGMENT

We thank Stewart Loh for use of his circular dichroism spectrometer.

SUPPORTING INFORMATION AVAILABLE

Table summarizing the data presented here, table of primers used for mutant construction, SDS−PAGE analysis of purified recombinant TEs, kinetic data, CD spectra, thermal denaturation curves, and a multiple-sequence alignment. This material is available free of charge via the Internet at http://pubs.acs.org.

REFERENCES

1. Wiley, P. F., Gerzon, K., Flynn, E. H., Sigal, M. V., Weaver, O., Quarck, U. C., Chauvette, R. R., and Monahan, R. (1957) Erythromycin. X. Structure of Erythromycin. *J. Am. Chem. Soc. 79*, 6062–6070.
2. Mao, J. C., and Wiegand, R. G. (1968) Mode of action of macrolides. *Biochim. Biophys. Acta 157*, 404–413.
3. Donadio, S., Staver, M. J., McAlpine, J. B., Swanson, S. J., and Katz, L. (1991) Modular organization of genes required for complex polyketide biosynthesis. *Science 252*, 675–679.
4. Golding, B. T., and Rickards, R. W. (1966) The structure of the macrolide antibiotic pimaricin. *Tetrahedron Lett.,* 3551–3557.
5. Aparicio, J. F., Fouces, R., Mendes, M. V., Olivera, N., and Martin, J. F. (2000) A complex multienzyme system encoded by five polyketide synthase genes is involved in the biosynthesis of the 26-membered polyene macrolide pimaricin in *Streptomyces natalensis*. *Chem. Biol. 7*, 895–905.
6. Gerth, K., Bedorf, N., Hofle, G., Irschik, H., and Reichenbach, H. (1996) Epothilons A and B: Antifungal and cytotoxic compounds from *Sorangium cellulosum* (Myxobacteria). Production, physicochemical and biological properties. *J. Antibiot. 49*, 560–563.
7. Tang, L., Shah, S., Chung, L., Carney, J., Katz, L., Khosla, C., and Julien, B. (2000) Cloning and heterologous expression of the epothilone gene cluster. *Science 287*, 640–642.
8. Molnar, I., Schupp, T., Ono, M., Zirkle, R., Milnamow, M., Nowak-Thompson, B., Engel, N., Toupet, C., Stratmann, A., Cyr, D. D., Gorlach, J., Mayo, J. M., Hu, A., Goff, S., Schmid, J., and Ligon, J. M. (2000) The biosynthetic gene cluster for the microtubule-stabilizing agents epothilones A and B from *Sorangium cellulosum* So ce90. *Chem. Biol. 7*, 97–109.
9. Kohli, R. M., and Walsh, C. T. (2003) Enzymology of acyl chain macrocyclization in natural product biosynthesis. *Chem. Commun.,* 297–307.
10. Boddy, C. N., Schneider, T. L., Hotta, K., Walsh, C. T., and Khosla, C. (2003) Epothilone C macrolactonization and hydrolysis are catalyzed by the isolated thioesterase domain of epothilone polyketide synthase. *J. Am. Chem. Soc. 125*, 3428–3429.
11. He, W. G., Wu, J. Q., Khosla, C., and Cane, D. E. (2006) Macrolactonization to 10-deoxymethynolide catalyzed by the recombinant thioesterase of the picromycin. *Bioorg. Med. Chem. Lett. 16*, 391–394.
12. Kopp, F., and Marahiel, M. A. (2007) Macrocyclization strategies in polyketide and nonribosomal peptide biosynthesis. *Nat. Prod. Rep. 24*, 735–749.
13. Aldrich, C. C., Venkatraman, L., Sherman, D. H., and Fecik, R. A. (2005) Chemoenzymatic synthesis of the polyketide macrolactone 10-deoxymethynolide. *J. Am. Chem. Soc. 127*, 8910–8911.
14. Gokhale, R. S., Hunziker, D., Cane, D. E., and Khosla, C. (1999) Mechanism and specificity of the terminal thioesterase domain from the erythromycin polyketide synthase. *Chem. Biol. 6*, 117–125.
15. Lu, H. X., Tsai, S. C., Khosla, C., and Cane, D. E. (2002) Expression, site-directed mutagenesis, and steady state kinetic analysis of the terminal thioesterase domain of the methymycin. *Biochemistry 41*, 12590–12597.

16. Sharma, K. K., and Boddy, C. N. (2007) The thioesterase domain from the pimaricin and erythromycin biosynthetic pathways can catalyze hydrolysis of simple thioester substrates. *Bioorg. Med. Chem. Lett. 17*, 3034–3037.
17. Weissman, K. J., Smith, C. J., Hanefeld, U., Aggarwal, R., Bycroft, M., Staunton, J., and Leadlay, P. F. (1998) The thioesterase of the erythromycin-producing polyketide synthase: Influence of acyl chain structure on the mode of release of substrate analogues from the acyl enzyme intermediates. *Angew. Chem., Int. Ed. 37*, 1437–1440.
18. Xue, Q., Ashley, G., Hutchinson, C. R., and Santi, D. V. (1999) A multiplasmid approach to preparing large libraries of polyketides. *Proc. Natl. Acad. Sci. U.S.A. 96*, 11740–11745.
19. Jacobsen, J. R., Hutchinson, C. R., Cane, D. E., and Khosla, C. (1997) Precursor-directed biosynthesis of erythromycin analogs by an engineered polyketide synthase. *Science 277*, 367–369.
20. Kao, C. M., McPherson, M., McDaniel, R. N., Fu, H., Cane, D. E., and Khosla, C. (1997) Gain of Function Mutagenesis of the Erythromycin Polyketide Synthase. 2. Engineered Biosynthesis of an Eight-Membered Ring Tetraketide Lactone. *J. Am. Chem. Soc. 119*, 11339–11340.
21. Kao, C. M., Luo, G. L., Katz, L., Cane, D. E., and Khosla, C. (1995) Manipulation of Macrolide Ring Size by Directed Mutagenesis of a Modular Polyketide Synthase. *J. Am. Chem. Soc. 117*, 9105–9106.
22. Jacobsen, J. R., Cane, D. E., and Khosla, C. (1998) Spontaneous priming of a downstream module in 6-deoxyerythronolide B synthase leads to polyketide biosynthesis. *Biochemistry 37*, 4928–4934.
23. Schetter, B., and Mahrwald, R. (2006) Modern aldol methods for the total synthesis of polyketides. *Angew. Chem., Int. Ed. 45*, 7506–7525.
24. Menzella, H. G., Reid, R., Carney, J. R., Chandran, S. S., Reisinger, S. J., Patel, K. G., Hopwood, D. A., and Santi, D. V. (2005) Combinatorial polyketide biosynthesis by de novo design and rearrangement of modular polyketide synthase genes. *Nat. Biotechnol. 23*, 1171–1176.
25. Kittendorf, J. D., and Sherman, D. H. (2006) Developing tools for engineering hybrid polyketide synthetic pathways. *Curr. Opin. Biotechnol. 17*, 597–605.
26. Staunton, J., and Weissman, K. J. (2001) Polyketide biosynthesis: A millennium review. *Nat. Prod. Rep. 18*, 380–416.
27. Walsh, C. T. (2002) Combinatorial biosynthesis of antibiotics: Challenges and opportunities. *ChemBioChem 3*, 125–134.
28. Bruner, S. D., Weber, T., Kohli, R. M., Schwarzer, D., Marahiel, M. A., Walsh, C. T., and Stubbs, M. T. (2002) Structural basis for the cyclization of the lipopeptide antibiotic surfactin by the thioesterase domain SrfTE. *Structure 10*, 301–310.
29. Pemble, C. W., IV, Johnson, L. C., Kridel, S. J., and Lowther, W. T. (2007) Crystal structure of the thioesterase domain of human fatty acid synthase inhibited by Orlistat. *Nat. Struct. Mol. Biol. 14*, 704–709.
30. Tsai, S. C., Miercke, L. J. W., Krucinski, J., Gokhale, R., Chen, J. C. H., Foster, P. G., Cane, D. E., Khosla, C., and Stroud, R. M. (2001) Crystal structure of the macrocycle-forming thioesterase domain of the erythromycin polyketide synthase: Versatility from a unique substrate channel. *Proc. Natl. Acad. Sci. U.S.A. 98*, 14808–14813.
31. Tsai, S. C., Lu, H. X., Cane, D. E., Khosla, C., and Stroud, R. M. (2002) Insights into channel architecture and substrate specificity from crystal structures of two macrocycle-forming thioesterases of modular polyketide synthases. *Biochemistry 41*, 12598–12606.
32. Giraldes, J. W., Akey, D. L., Kittendorf, J. D., Sherman, D. H., Smith, J. L., and Fecik, R. A. (2006) Structural and mechanistic insights into polyketide macrolactonization from polyketide-based affinity labels. *Nat. Chem. Biol. 2*, 531–536.
33. Akey, D. L., Kittendorf, J. D., Giraldes, J. W., Fecik, R. A., Sherman, D. H., and Smith, J. L. (2006) Structural basis for macrolactonization by the pikromycin thioesterase. *Nat. Chem. Biol. 2*, 537–542.
34. Qian, Z., Fields, C. J., Yu, Y., and Lutz, S. (2007) Recent progress in engineering α/β hydrolase-fold family members. *Biotechnol. J. 2*, 192–200.
35. Sambrook, J. F., and Russell, D. W., Eds. (2000) *Molecular cloning: A laboratory manual*, 3rd ed., Cold Spring Harbor Laboratory Press, Plainview, NY.
36. Kustedjo, K., Deechongkit, S., Kelly, J. W., and Cravatt, B. F. (2003) Recombinant expression, purification, and comparative characterization of torsinA and its torsion dystonia-associated variant ΔE-torsinA. *Biochemistry 42*, 15333–15341.
37. Koepf, E. K., Petrassi, H. M., Sudol, M., and Kelly, J. W. (1999) WW: An isolated three-stranded antiparallel β-sheet domain that unfolds and refolds reversibly: Evidence for a structured hydrophobic cluster in urea and GdnHCl and a disordered thermal unfolded state. *Protein Sci. 8*, 841–853.
38. Pazirandeh, M., Chirala, S. S., and Wakil, S. J. (1991) Site-directed mutagenesis studies on the recombinant thioesterase domain of chicken fatty acid synthase expressed in *Escherichia coli*. *J. Biol. Chem. 266*, 20946–20952.
39. Witkowski, A., Witkowska, H. E., and Smith, S. (1994) Reengineering the specificity of a serine active-site enzyme. Two active-site mutations convert a hydrolase to a transferase. *J. Biol. Chem. 269*, 379–383.
40. Li, J., Szittner, R., Derewenda, Z. S., and Meighen, E. A. (1996) Conversion of serine-114 to cysteine-114 and the role of the active site nucleophile in acyl transfer by myristoyl-ACP thioesterase from *Vibrio harveyi*. *Biochemistry 35*, 9967–9973.
41. Nardini, M., and Dijkstra, B. W. (1999) α/β hydrolase fold enzymes: The family keeps growing. *Curr. Opin. Struct. Biol. 9*, 732–737.
42. Fersht, A. (1998) *Structure and Mechanism in Protein Science: A Guide to Enzyme Catalysis and Protein Folding*, W. H. Freeman, New York.
43. Fasman, G. D., Ed. (1996) *Circular Dichroism and the Conformational Analysis of Biomolecules*, Plenum Press, New York.
44. Xue, Y., Zhao, L., Liu, H. W., and Sherman, D. H. (1998) A gene cluster for macrolide antibiotic biosynthesis in *Streptomyces venezuelae*: Architecture of metabolic diversity. *Proc. Natl. Acad. Sci. U.S.A. 95*, 12111–12116.
45. Kakavas, S. J., Katz, L., and Stassi, D. (1997) Identification and characterization of the niddamycin polyketide synthase genes from *Streptomyces caelestis*. *J. Bacteriol. 179*, 7515–7522.
46. Castonguay, R., He, W., Chen, A. Y., Khosla, C., and Cane, D. E. (2007) Stereospecificity of ketoreductase domains of the 6-deoxyerythronolide B synthase. *J. Am. Chem. Soc. 129*, 13758–13769.
47. Roujeinikova, A., Simon, W. J., Gilroy, J., Rice, D. W., Rafferty, J. B., and Slabas, A. R. (2007) Structural studies of fatty acyl-(acyl carrier protein) thioesters reveal a hydrophobic binding cavity that can expand to fit longer substrates. *J. Mol. Biol. 365*, 135–145.
48. Leibundgut, M., Jenni, S., Frick, C., and Ban, N. (2007) Structural basis for substrate delivery by acyl carrier protein in the yeast fatty acid synthase. *Science 316*, 288–290.
49. Tran, L., Tosin, M., Spencer, J. B., Leadlay, P. F., and Weissman, K. J. (2008) Covalent Linkage Mediates Communication between ACP and TE Domains in Modular Polyketide Synthases. *ChemBioChem 9*, 905–915.
50. Song, F., Zhuang, Z., and Dunaway-Mariano, D. (2007) Structure-activity analysis of base and enzyme-catalyzed 4-hydroxybenzoyl coenzyme A hydrolysis. *Bioorg. Chem. 35*, 1–10.
51. Stivers, J. T., and Nagarajan, R. (2006) Probing enzyme phosphoester interactions by combining mutagenesis and chemical modification of phosphate ester oxygens. *Chem. Rev. 106*, 3443–3467.
52. Elgavish, S., and Shaanan, B. (1997) Lectin-carbohydrate interactions: Different folds, common recognition principles. *Trends Biochem. Sci. 22*, 462–467.
53. Ohtaki, A., Iguchi, A., Mizuno, M., Tonozuka, T., Sakano, Y., and Kamitori, S. (2003) Mutual conversion of substrate specificities of *Thermoactinomyces vulgaris* R-47 α-amylases TVAI and TVAII by site-directed mutagenesis. *Carbohydr. Res. 338*, 1553–1558.
54. Wada, M., Hsu, C. C., Franke, D., Mitchell, M., Heine, A., Wilson, I., and Wong, C. H. (2003) Directed evolution of N-acetylneuraminic acid aldolase to catalyze enantiomeric aldol reactions. *Bioorg. Med. Chem. 11*, 2091–2098.
55. Hsu, C. C., Hong, Z., Wada, M., Franke, D., and Wong, C. H. (2005) Directed evolution of D-sialic acid aldolase to L-3-deoxy-manno-2-octulosonic acid (L-KDO) aldolase. *Proc. Natl. Acad. Sci. U.S.A. 102*, 9122–9126.

BI800963Y